

Effect of anodization and alkali-heat treatment on the bioactivity of titanium implant material (an *in vitro* study)

Ramy A. Abdelrahim^{1,2}, Nadia A. Badr³, Kusai Baroudi⁴

¹Department of Dental Biomaterials, School of Dentistry, Al-Azhar University, ³Department of Dental Biomaterials, Faculty of Oral and Dental Medicine, Cairo University, Egypt, Departments of ²Restorative Dental Sciences and ⁴Preventive Dental Sciences, Alfarabi Colleges, Riyadh, Kingdom of Saudi Arabia

Corresponding author (email: <d_kusai@yahoo.co.uk>)

Dr. Kusai Baroudi, Department of Preventive Dental Sciences, Alfarabi Colleges, P. O. Box: 85184, Riyadh 11691, Kingdom of Saudi Arabia.

Received: 04-01-16

Accepted: 04-04-16

Published: 30-05-16

Abstract

Objective: This study was aimed to assess the effect of anodized and alkali-heat surface treatment on the bioactivity of titanium alloy (Ti-6Al-4V) after immersion in Hank's solution for 7 days. **Materials and Methods:** Fifteen titanium alloy samples were used in this study. The samples were divided into three groups (five for each), five samples were anodized in 1M H₃PO₄ at constant voltage value of 20 v and another five samples were alkali-treated in 5 M NaOH solution for 25 min at temperature 60°C followed by heat treatment at 600°C for 1 h. All samples were then immersed in Hank's solution for 7 days to assess the effect of surface modifications on the bioactivity of titanium alloy. The different treated surfaces and control one were characterized by X-ray diffraction, atomic force microscopy, scanning electron microscopy, energy-dispersive X-ray spectroscopy, and Fourier transformation infra-red spectroscopy. Statistical analysis was performed with PASW Statistics 18.0® (Predictive Analytics Software). **Results:** Anodization of Ti-alloy samples (Group B) led to the formation of bioactive titanium oxide anatase phase and PO₄³⁻ group on the surface. The alkali-heat treatment of titanium alloy samples (Group C) leads to the formation of bioactive titania hydrogel and supplied sodium ions. The reaction between the Ti sample and NaOH alkaline solution resulted in the formation of a layer of amorphous sodium titania on the Ti surface, and this layer can induce apatite deposition. **Conclusions:** The surface roughness and surface chemistry had an excellent ability to induce bioactivity of titanium alloy. The anodization in H₃PO₄ produced anatase titanium oxide on the surface with phosphate originated from electrolytes changed the surface topography and allowed formation of calcium-phosphate.

Key words: Alkali-heat treatment, anodization, bioactivity, surface roughness

INTRODUCTION

Titanium and its alloys widely used as implant biomaterials because of their relatively superior physical properties such as lower modulus, low density, and relatively low elastic modulus and because of

their superior biocompatibility due to their excellent corrosion resistance, and bioinertness of the oxide layer.^[1,2] Therefore, titanium (Ti) and its alloys mainly (Ti-6Al-4V) became the most suitable metal for endosseous implants fabrication.^[3,4]

Access this article online	
Quick Response Code:	Website: www.jispcd.org
	DOI: 10.4103/2231-0762.183107

This is an open access article distributed under the terms of the Creative Commons Attribution-NonCommercial-ShareAlike 3.0 License, which allows others to remix, tweak, and build upon the work non-commercially, as long as the author is credited and the new creations are licensed under the identical terms.

For reprints contact: reprints@medknow.com

How to cite this article: Abdelrahim RA, Badr NA, Baroudi K. Effect of anodization and alkali-heat treatment on the bioactivity of titanium implant material (an *in vitro* study). J Int Soc Prevent Communit Dent 2016;6:189-95.

One of the most serious and prevalent mechanisms, for obtaining biofunctional and biocompatible material for biomedical use, is surface modification. The surface modification technique is a process that changes the material surface through changes in their chemical composition, structure, and morphology, but the bulk mechanical properties of the material not affected.^[5,6]

The surface of a biomaterial plays a key role in determining biocompatibility.^[7,8] Therefore, biomaterials surface in contact with the biological tissue or fluid is named “biointerface.”^[9] The biointerface is the place where the modifications are commonly carried out to make biomaterials more compatible, and these modifications are fall under three categories, namely, morphologic, physicochemical, and biological. Surface of biomaterials represents a crucial value for biomedical field and determine biocompatibility of the biomaterial because only the uppermost molecular layers are in intimate contact with the biological environment.^[10] Thus, any interaction between the implant materials and the biological environment occurs at or through the level of narrow zone termed as the interface. Therefore, the biomaterial scientists have a special concern with the interfacial chemistry that determined by the uppermost few nanometers that composed the materials surface.^[10]

For an optimally bonding between the implant material and living bone in the human body, it is essential that the implant can form bone-like apatite layer on its surface. The nucleation of apatite on the surface of a material is induced by the functional groups on its surface.^[11,12] The surface modification of titanium implants is an interested issue for investigation aiming to induce acceleration of normal bone healing allowing immediate loading of the implant.^[11,12]

The treatment of titanium surfaces by alkaline solution followed by heat treatment was described by some investigators,^[13-16] who successfully proved the bioactive induction both *in vitro*^[17] and *in vivo*.^[18] Hydroxyapatite formation onto Ti surface can be accelerated by treatment titanium surface by NaOH solution followed by heat treatment to produce layer of sodium titanate on titanium surface. Titanium surface that treated with alkaline solution followed heat treatment is thought to bond to living bone via formation of apatite layer on its surface while the titanium surface that treated with alkaline solution only did not.^[13,14] Recently, *in vitro* studies showed that bone-like apatite could be formed on the titanium surface that treated with alkaline followed by heat treatment when immersed in simulating body fluid (SBF) via formation of titana hydrogel on titanium surface.^[13,14]

Among surface treatments, the anodizing exhibited effectiveness in modifying surface properties of metals,^[19] particularly in inducing the bioactivity of titanium.^[20] Anodic oxidation of titanium implants involved several changes in oxide characteristic increases not only the thickness of native oxide layer but also the surface texture such as the ability of fabricating porous Ti oxide films, the changeability of the crystalline structure, chemical composition of oxide film, and through formation of rough and homogeneous TiO₂ layer with numerous nanoscale pores.^[20] The surface modification of titanium implants by anodic oxidation in phosphoric/sulfuric acid electrolyte systems showed an increase in oxide thickness,^[20] which significantly improves the bone response for better osseointegration between Ti surface and surrounding bone.^[21]

This study aimed to investigate the effect of different surface treatment on the bioactivity of titanium alloy (Ti-6Al-4V) and their ability to form calcium phosphate apatite crystals on their surfaces after immersion in a simulated body fluid.

MATERIALS AND METHODS

This study was performed in the Department of Biomaterials, Faculty of Dental Medicine, Al-Azhar University. Ethical approval of Al-Azhar University was taken (under number 207/2009).

A total of fifteen samples made of Ti-6Al-4V alloy (extra low interstitials F 130-84 alloy, USA) were used in this study. The sample dimensions were rectangular in shape of 15 mm in length, 7 mm in width, and 2 mm in thickness. The titanium samples were silky polished using sandpaper starting from gravel #400 to #1200, and then ultrasonically cleaned in deionized water for 5 min before dried by air dryer.

Then, the samples were classified into three groups according to the following treatments: Five sample each, according to the received surface treatment. The surface treatment involved anodization (Group B) and alkali-heat treatment (Group C). Five samples were kept untreated and served as control (Group A). Ten samples of Groups B and C were etched in acid blend of 80 ml/l HNO₃, 60 ml/l HF, and 150 ml/l H₂O₂ for 5 min at room temperature before the surface treatment.

Five samples were subjected to anodization process, Group B, after acid etching to form an oxide porous film on their surfaces. The anodizing processes were performed in electrochemical cell that has an anodizing

solution as electrolyte and two electrodes using a direct current source with value of 20 v as constant voltage. A cathode of platinum is connected to the negative terminal of a voltage source and placed in the solution, and Ti-alloy sample is connected to the positive terminal of the voltage source and also place in the solution as anode with about 4 cm as a fixed distance between cathode and anode. An electrolyte bath consists of 98 g/L (1 M H_3PO_4) aqueous solution (1 L total volume) having pH 1.5 that was stirred with magnetic stirrer with 180 rpm. The anodizing process was carried out at room temperature for 15 min, and then the samples were ultrasonically cleaned for 5 min in deionized water.

The samples of Group C were alkali-treated by immersion in 5 M NaOH solution for 25 min at temperature 60°C and washed with distilled water, and dried in the air. Then, the samples were heat treated at 600°C for 1 h in a furnace at heating rate 30°C/min. Then, they gradually cooled to room temperature.

The surfaces of each group were characterized after surface treatment using X-ray diffraction (XRD) (Philips Analytical X-ray B.V.), scanning electron microscopy (SEM) (Technics Inc., JEOL JSM 5410, Japan production), and atomic force microscopy (Thermomicroscopes Autoprobe CP research, scanner 100 m, USA).

Before immersion in Hank's balanced salt solution (HBSS), the samples were rinsed with distilled water, washed further with ethanol in an ultrasonic bath for 20 min, and then dried in air. All the investigated samples were immersed for 7 days in the HBSS which was used as SBF at pH 7.4 and 37°C. HBSS was renewed every 3 days to maintain the level of ion concentration allowing for biomimetic coat precipitation on the sample surfaces. After the immersion of the Ti-alloy samples in HBSS, the specimens were removed from the solution, gently rinsed with distilled water and then dried at 60°C for 24 h.

To assess the biomimetic coat on the differently treated samples, microstructural/morphological changes of the specimens' surfaces were characterized. Meanwhile, the surface morphology was examined using SEM. Energy dispersive X-ray analysis (EDXA) (Model: Link ISIS-OXFORD – England. The device is attached to JEOL-5400 Scanning Microscope) assembled on the SEM was used to determine the atomic % of calcium, phosphorous elements, and Ca/P ratio of

the precipitation. Fourier transformation infra-red spectroscopy (FTIR) (FT/6300 Type A. Jasco, Japan) was used to analyze qualitatively the chemical structure of biomimetic coat which precipitated on the immersed surface.

Statistical analysis

Statistical analysis was performed using one-way ANOVA followed by Tukey's *post hoc* test at the significance level of $\alpha = 0.05$.

RESULTS

The XRD analysis of the anodized group revealed the presence of anatase TiO_2 phase while the alkali-heat-treated group reveals the presence of rutile TiO_2 and Ti-OH phases as shown in Figure 1.

Atomic Force Micrograph of the alkali-heat treated group shows the highest surface roughness among the all investigated group with multiple deep valises in three-dimensional (3D) image, followed by the anodized group, which shows severe undulation of the surface; however, no sharp peaks were evident in the 3D images and the least surface roughness was the control group, and its 3D image shows slight irregularities and serration of the metal surface due to polishing as shown in Figure 2.

The statistical analysis of the surface roughness of the different surface treated groups is shown in Figure 3. ANOVA test showed that there was a statistically significant difference among mean (Ra) values of the investigated groups with $P < 0.05$. Pair-wise comparisons among the groups revealed that alkali-heat-treated group showed the highest statistically significantly mean (Ra) value.

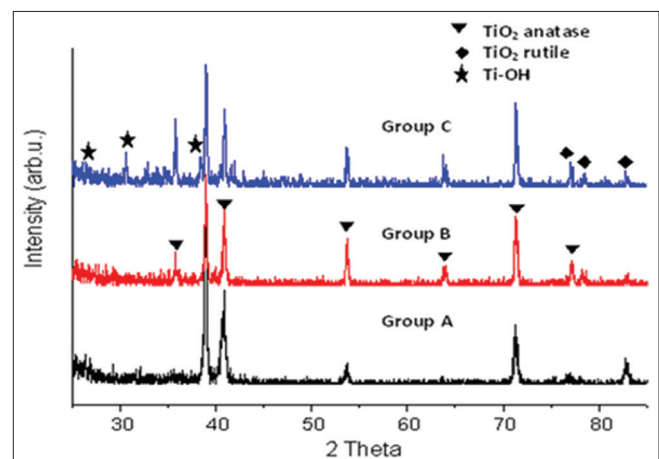


Figure 1: X-ray diffraction pattern of all investigated groups

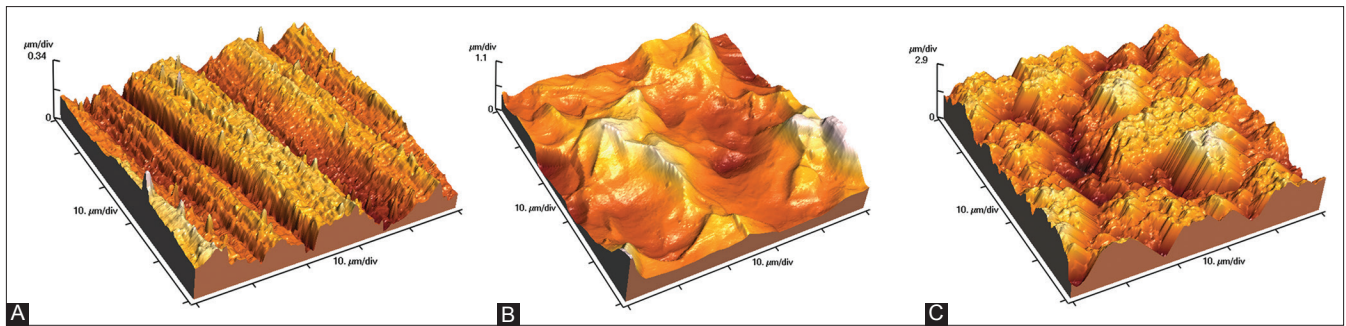


Figure 2: Atomic force micrographs of Group A, B, and C (three-dimensional)

The scanning electron micrograph of the control group showed that polishing marks of Ti-alloy obviously seen on the sample surface, and the anodized group revealed presence of numerous and unattached, well-defined, nano-sized pores while the alkali-heat-treated group revealed the presence of numerous, unattached, well-defined, nano-sized pores that arranged in an ordered pattern and equally distributed all over the structure on the surface spread among micro-sized particles. It was prominent that the pores are deeper with darker contrast [Figure 4].

After immersion in Hank's solution, the SEM showed discrete small apatite crystals formed on the surface of the control samples and the EDXA spectrum showed phosphorus atomic% of 53.94 and calcium atomic% of 46.05 and Ca/P ratio of 0.85, which is much lower than stoichiometric value of hydroxyapatite (1.67). It indicates the synthesis of mono-calcium phosphate monohydrate of chemical composition of $\text{Ca}(\text{H}_2\text{PO}_4)_2 \cdot \text{H}_2\text{O}$ and/or dicalcium phosphate dehydrate (brushite) $\text{CaHPO}_4 \cdot 2\text{H}_2\text{O}$ [Figures 4-II and 5].

The SEM of the anodized group showed contiguous layer of apatite nuclei formed on the surface of the anodized samples such that the substrate is not obviously seen and EDXA spectrum showed phosphorus atomic% of 43.72 and calcium atomic% of 56.28 and Ca/P ratio of 1.28, which is less than stoichiometric value of hydroxyapatite (1.67). This ratio indicates the synthesis of octacalcium phosphate of chemical composition $\text{Ca}_8(\text{HPO}_4)_2(\text{PO}_4)_4 \cdot 5\text{H}_2\text{O}$ [Figures 4-II and 5].

While the SEM of the alkali-heat-treated group exhibited layer composed of an interconnected spherical particle, this layer is to some extent thicker, and the particles are larger in size. The EDXA spectrum showed phosphorus atomic% of 37.96 and calcium atomic% of 62.04 and Ca/P ratio of 1.67. This ratio suggests the formation of calcium deficient hydroxyapatite

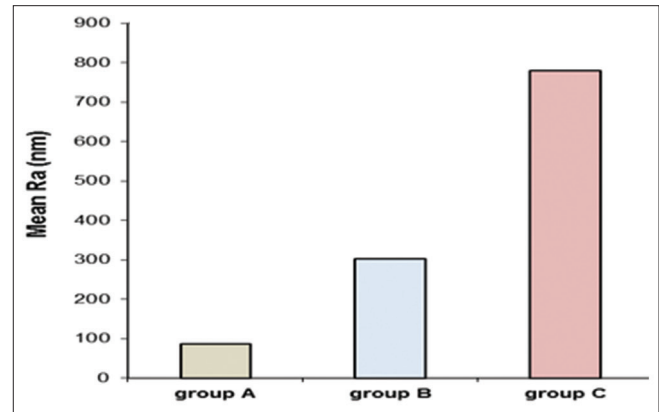


Figure 3: Mean values of surface roughness (Ra) of the investigated groups

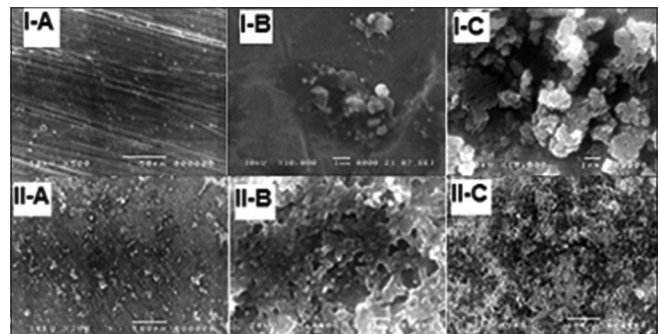


Figure 4: Scanning electron micrographs of Group A, B, and C before and after immersion in Hank's solution

or occasionally named precipitated HA of chemical formula $\text{Ca}_x \text{H}_y (\text{PO}_4)_z \cdot n\text{H}_2\text{O}$ [Figures 4-II and 5].

The FTIR analysis of control group, Group A, is shown in Figure 6. The spectrum revealed that the presence of vibration band at 606 cm^{-1} is for symmetric stretching vibration of PO_4^{3-} (ν_4). The bands at 865 and 985 cm^{-1} are bands for symmetric stretching vibration of PO_4^{3-} (ν_1) while band at 1019 cm^{-1} for asymmetric stretching vibrations of PO_4^{3-} (ν_3). The symmetric stretching vibrations of PO_4^{3-} (ν_3) are represented by bands at 1058 and 1090 cm^{-1} while the band at 1075 cm^{-1} is absent. The symmetric stretching vibration

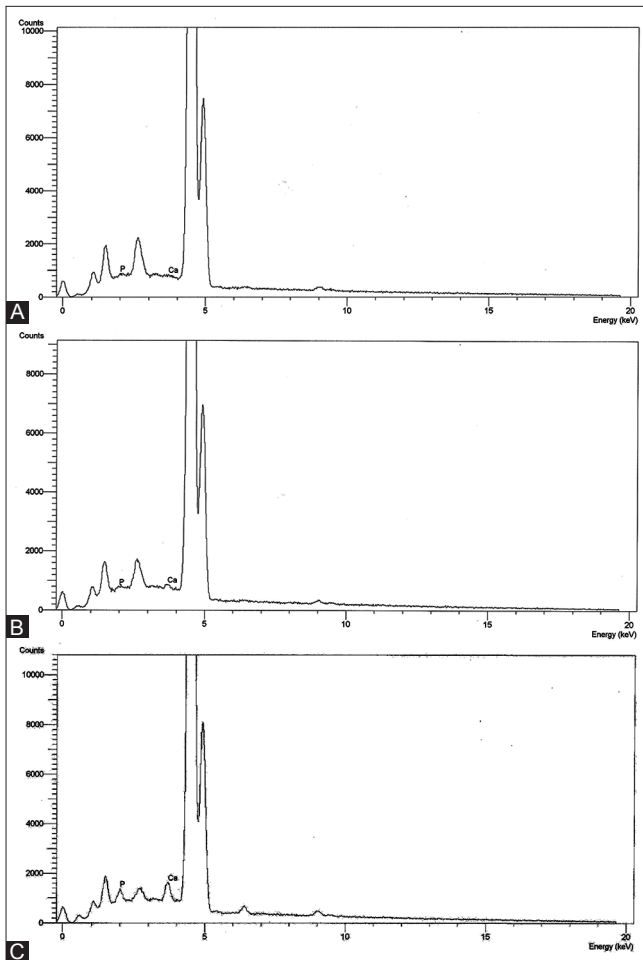


Figure 5: Energy-dispersive X-ray spectrum of group A, B and C after immersion in Hank's solution

bands of HPO_4^{2-} group are observed at 1113, 1141 and 1226 cm^{-1} . The symmetric stretching vibration bands of CO_3^{2-} are captured at 873, 1414, and 1453 cm^{-1} . The reflectance bands characteristic for H_2O were observed at 625, 3083, 3249, 3333, and 3546 cm^{-1} which denoting OH^- group of HA. The carbonyl group $\text{C}=\text{O}$ is identified from bands at 1698 and 1712 cm^{-1} .

The FTIR analysis of anodized samples, Group B, is shown in Figure 6. The spectrum revealed that the presence of vibration bands at 563 and at 604 cm^{-1} is for symmetric stretching vibrations of PO_4^{3-} (ν_4). The bands at 862 and 965 cm^{-1} are bands for symmetric stretching vibration of PO_4^{3-} (ν_1) while band at 1020 cm^{-1} is for asymmetric stretching vibrations of PO_4^{3-} (ν_3). The symmetric stretching vibrations of PO_4^{3-} (ν_3) are represented by band 1076 cm^{-1} while the band at 1047 and at 1096 is absent. The symmetric stretching vibration bands of HPO_4^{2-} group are observed at 1114, 1143, and 1222 cm^{-1} . The symmetric stretching vibration bands of CO_3^{2-} are captured at 875, 1416, and

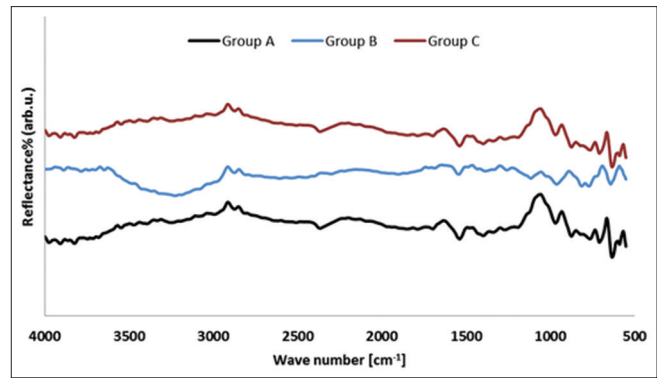


Figure 6: Fourier transformation infra-red spectroscopy spectra of investigated Groups A, B, and C after immersion in Hank's solution

1455 cm^{-1} . The reflectance bands characteristic for H_2O are observed at 629 and 3230 cm^{-1} which denoting OH^- group of HA. A broad and not very intense band in HAP at 3230 cm^{-1} may be due to the presence of lattice water in the solid or it caused by the H-bonding between the adsorbed H_2O and the OH group of the apatite. The carbonyl group $\text{C}=\text{O}$ is identified from bands at 1693 and 1760 cm^{-1} .

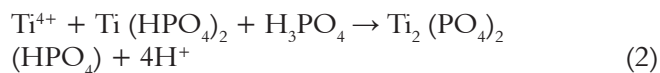
The FTIR analysis of alkali-heat-treated samples, Group C, is shown in Figure 6. The spectrum revealed that the presence of vibration bands at 561 and at 602 cm^{-1} is for symmetric stretching vibration of PO_4^{3-} (ν_4) while bands at 871, 960, and 985 cm^{-1} are characteristic bands for symmetric stretching vibration of PO_4^{3-} (ν_1) while band at 1019 cm^{-1} is characteristic for asymmetric stretching vibrations of PO_4^{3-} (ν_3). The symmetric stretching vibrations of PO_4^{3-} (ν_3) are represented by band 1093 cm^{-1} while the band at 1048 and 1075 cm^{-1} is absent. The symmetric stretching vibration bands of HPO_4^{2-} group are observed at 1111 and 1220 cm^{-1} . The symmetric stretching vibration bands of CO_3^{2-} are captured at 1416 and 1455 cm^{-1} . The reflectance bands characteristic for H_2O were observed at 626, 3001, 3195, and 3550 cm^{-1} which denoting OH^- group of HA. The carbonyl Group $\text{C}=\text{O}$ is identified from bands at 1712, 1726 cm^{-1} .

DISCUSSION

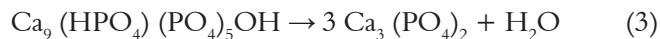
The anodization in H_3PO_4 produced anatase titanium oxide on the surface with phosphate originated from electrolytes and changed the surface topography.^[22,23] In addition, crystal structures of titanium oxide found on titanium surface after anodization^[24,25] allowed formation of calcium-phosphate in Hank's solution with ion concentrations approximating those of human blood plasma.^[26]

It is reported that in aqueous body fluid, the OH⁻ bonds easily to the Ti⁴⁺ of TiO₂ and subsequently Ti-OH groups is formed.^[27] The isoelectric point of titanium oxide surface at electrolyte pH nearly 5–6 shows zero net charge. A positively charged surface will be created by production of (Ti-OH₂)⁺ in the surface layer at electrolyte pH <5. The Ti-OH will be deprotonated at electrolyte pH >6, and becomes (Ti-OH)⁻ so the surface will be a negatively charged. Therefore, the surface will be negatively charged at the physiological pH of ~7.4, due to the existence of deprotonated acidic hydroxides.^[28] That negatively charged surface can attract cations such as calcium that subsequently could react with HPO₄²⁻ or H₂PO₄⁻ to form calcium phosphates.^[29]

The titanium cations can react with phosphoric acid to form phosphates as explained in the following reactions:



In turn, the nucleation of calcium phosphate nanocrystals within nanopores could be facilitated by the presence of these phosphate ions.^[30]



The reaction between the Ti sample and NaOH alkaline solution will lead to the formation of a layer of amorphous sodium titania on the Ti surface. Alkaline treatment for 25 min would provide a titania layer of considerable thickness with mature submicrometer porosity. Further, heat treatment at temperature (600°C) for extended time (1 h) resulted in a cracked layer with an increased thickness. The thickness and gradual transformation of the titania layer from an amorphous to a crystalline state depended almost linearly on the period and the temperature of the chemical treatment.^[31]

This layer can induce apatite deposition in SBF by a mechanism was proposed by Cui and Kim 2008. Their elucidation based on the reaction of Na⁺ ions from sodium titanate layer, with H₃O⁺ ions forming Ti-OH groups on the surface. Those Ti-OH groups on the titanium surface are essential for the formation of calcium phosphates. These negatively charged Ti-OH groups react with positively charged Ca²⁺ ions from the SBF and form calcium titanate, which acts as nucleation sites for apatite crystal formation. Therefore, the more Ti-OH groups, the more would be the ability to induce

apatite nucleation. On accumulation of Ca²⁺ ions, the calcium titanate changed to be positively charged and combined with negatively charged phosphate to form calcium phosphates and then transform to apatite.^[32]

The difference between the surface activities of chemically and electrochemically treated Ti-6Al-4V is due to the different surface morphology and structure, i.e., increased surface roughness lead to increased bioactivity.^[33,34]

Limitations

Although this research was carefully prepared, I am still aware of its limitations and shortcomings.

First of all, the research was concerned only with *in vitro* and have not any *in vivo* study.

Second, the study did not cover different surface modification methods.

Third, the study was done using titanium alloy discs and not titanium implants.

CONCLUSIONS

Electrochemical treatment of anodic oxidation in H₃PO₄ solution converted titanium oxide to the favorable anatase phase and provided PO₄³⁻ which acted as nuclei for developing HA crystals. Immersion in NaOH solution before alkali-heat treatment of titanium alloy supplied sodium ions and titania hydrogel which are beneficial substrate to precipitate calcium and phosphorus in a ratio comparable to that of stoichiometric HA.

Financial support and sponsorship

Nil.

Conflicts of interest

There are no conflicts of interest.

REFERENCES

1. Liu X, Chu PK, Ding C. Surface modification of titanium, titanium alloys, and related materials for biomedical applications. *Mater Sci Eng* 2004;47:49-121.
2. Wally ZJ, Grunsven WV, Claeysens F, Goodall R, Reilly GC. Porous titanium for dental implant applications (Review Article). *Metals* 2015;5:1902-20.
3. Lautenschlager EP, Monaghan P. Titanium and titanium alloys as dental materials. *Int Dent J* 1993;43:245-53.
4. Özcan M, Hämmerle C. Titanium as a reconstruction and

- implant material in dentistry: Advantages and pitfalls. *Materials* 2012;5:1528-45.
5. Hanawa T. An overview of biofunctionalization of metals in Japan. *Soc Interface J* 2009;6:S361-9.
 6. Jemat A, Ghazali MJ, Razali M, Otsuka Y. Surface modifications and their effects on titanium dental implants (Review Article). *Bio Med Res Int* 2015;10:1155-66.
 7. Hallab NJ, Bundy KJ, O'Connor K, Moses RL, Jacobs JJ. Evaluation of metallic and polymeric biomaterial surface energy and surface roughness characteristics for directed cell adhesion. *Tissue Eng* 2001;7:55-71.
 8. Seon GM, Seo HJ, Kwon SY, Lee MH, Kwon BJ, Kim MS, *et al.* Titanium surface modification by using microwave-induced argon plasma in various conditions to enhance osteoblast biocompatibility. *Biomater Res* 2015;19:13.
 9. Rao KS, Panda AK, Labhasetwar V. Intravascular drug delivery systems and devices: Interactions at biointerface. *Surf Interface Biomater* 2005;(2005):573-83.
 10. Vogler EA. Interfacial chemistry in biomaterials science, in wettability. *Surfactant Sci Ser* 1993;49:184-250.
 11. Uchida M, Kim HM, Kokubo T, Miyaji F, Nakamura T. Bonelike apatite formation induced on zirconia gel in a simulated body fluid and its modified solutions. *J Am Ceram Soc* 2001;84:2041-4.
 12. Kurella A, Dahotre NB. Review paper: Surface modification for bioimplants: The role of laser surface engineering. *J Biomater Appl* 2015;29(7):915-28.
 13. Kim HM, Miyaji F, Kokubo T, Nakamura T. Preparation of bioactive Ti and its alloys via simple chemical surface treatment. *J Biomed Mater Res* 1996;32:409-17.
 14. Kokubo T, Yamaguchi S. Bioactive titanate layers formed on titanium and its alloys by simple chemical and heat treatments. *Open Biomed Eng J* 2015;9:29-41.
 15. Liang FH, Zhou L, Wang KG. Influence of heat treatment on the *in vitro* bioactivity of alkali-treated titanium surfaces. *Surf Coat Technol* 2003;165:133-39.
 16. Bsat S, Yavari SA, Munsch M, Valstar ER, Zadpoor AA. Effect of alkali-acid-heat chemical surface treatment on electron beam melted porous titanium and its apatite forming ability. *Materials* 2015;8:1612-25.
 17. Xing H, Komasa S, Taguchi Y, Sekino T, Okazaki J. Osteogenic activity of titanium surfaces with nanonetwork structures. *Int J Nanomedicine* 2014;9:1741-55.
 18. So K, Kaneuji A, Matsumoto T, Matsuda S, Akiyama H. Is the bone-bonding ability of a cementless total hip prosthesis enhanced by alkaline and heat treatments? *Clin Orthop Relat Res* 2013;471:3847-55.
 19. Kim K, Lee BA, Piao XH, Chung HJ, Kim YJ. Surface characteristics and bioactivity of an anodized titanium surface. *J Periodontal Implant Sci* 2013;43:198-205.
 20. Krasicka-Cydzik E. Gel-like layer development during formation of thin anodic films on titanium in phosphoric acid solutions. *Corros Sci* 2004;46:2487-502.
 21. Kim MH, Park K, Choi KH, Kim SH, Kim SE, Jeong CM, *et al.* Cell adhesion and *in vivo* osseointegration of sandblasted/acid etched/anodized dental implants. *Int J Mol Sci* 2015;16:10324-36.
 22. Chrzanowski W. Corrosion study of Ti6Al7Nb alloy after thermal, anodic and alkali surface treatments. *J Achiev Mater Manuf Eng* 2008;31:2-6.
 23. Shabani M, Zamiri R, Goodarzi M. Study on the surface modification of titanium alloy by nanostructure TiO₂ grown through anodic oxidation treatment. *Austin Chem Eng* 2015;2:1015-20.
 24. Kim KH, Ramaswamy N. Electrochemical surface modification of titanium in dentistry. *Dent Mater J* 2009;28:20-36.
 25. Sanchez AG, Schreiner W, Duffó G, Ceré S. Surface modification of titanium by anodic oxidation in phosphoric acid at low potentials. Part 1. Structure, electronic properties and thickness of the anodic films. *Surf Interface Anal* 2013;45:1036-47.
 26. Gugelmina BS, Santosa LS, Ponte HA, Marinoc CE. Electrochemical stability and bioactivity evaluation of Ti6Al4V surface coated with thin oxide by EIS for biomedical applications. *Mater Res* 2015;18:602-7.
 27. Ma QQ, Li MH, Hu ZY, Chen Q, Hu WY. Enhancement of the bioactivity of titanium oxide nanotubes by precalcification. *J Mater Lett* 2008;62:3035-8.
 28. Rohanizadeh R, Al-Sadeq M, Legeros RZ. Preparation of different forms of titanium oxide on titanium surface: Effects on apatite deposition. *J Biomed Mater Res A* 2004;71:343-52.
 29. Kunze J, Müller L, Macak JM, Greil P, Schmuki P, Müller FA. Time-dependent growth of biomimetic apatite on anodic TiO₂ nanotubes. *Electrochim. J Acta Mater* 2008;53:6995-7003.
 30. Dorozhkin SV, Epple M. Biological and medical significance of calcium phosphates. *Angew Chem Int Ed Engl* 2002;41:3130-46.
 31. Wei M, Kim HM, Kokubo T, Evans JH. Optimising the bioactivity of alkaline treated titanium alloy. *Mater Sci Eng Coat* 2002;20:125-34.
 32. Cui X, Kim HM, Kawashita M, Wang L, Xiong T, Kokubo T, *et al.* Effect of hot water and heat treatment on the apatite-forming ability of titania films formed on titanium metal via anodic oxidation in acetic acid solutions. *J Mater Sci Mater Med* 2008;19:1767-73.
 33. Thirugnanam A, Kumar TS, Chakkingal U. Bioactivity enhancement of commercial pure titanium by chemical treatments. *Trends Biomater Artif Organs* 2009;22:202-10.
 34. Lindahl C, Engqvist H, Xia W. Influence of surface treatments on the bioactivity of Ti. *ISRN Biomater* 2013;(2013):19-28.